JOURNAL OF Materials CHEMISTRY

Random inorganic networks: a novel class of high-performance ceramics†

Leo van Wüllen and Martin Jansen*

Max-Planck-Institut für Festkörperforschung, Heisenbergstrasse 1, Stuttgart D-70569, Germany

Received 2nd May 2000, Accepted 10th July 2000
First published as an Advance Article on the web 5th October 2000

The preparation of amorphous inorganic networks in the system Si/B/N/C, starting from molecular single source precursors, results in high performance ceramics with outstanding and unprecedented high temperature and mechanical properties. Different ways of incorporating carbon into the final ceramics are described and new single source precursors presented. The local structure and intermediate range order in these amorphous inorganic networks are studied using conventional multinuclear ^{11}B, ^{13}C and ^{29}Si magic angle spinning (MAS) NMR and advanced double resonance techniques such as ^{29}Si-$\{^{11}B\}$ rotational echo adiabatic passage double resonance (REAPDOR), ^{13}C-$\{^{11}B\}$ REAPDOR or ^{11}B-$\{^{29}Si\}$ rotational echo double resonance (REDOR) NMR spectroscopy.

Introduction

Multinary nitridic ceramics that are processed by polycondensation of molecular precursors represent a rather new type of material.[1] Compared to conventional ceramics such as aluminosilicates and binary carbides and nitrides, the high temperature properties in particular are remarkably improved. As early as the late 1960s, Winter *et al.* were able to process fibers in the system Si/N/C by ammonolysis of methylchlorosilanes.[2,3] Since the mid 1970s ceramic fibers have been obtained on an industrial scale *via* the carbosilane route of Yajima *et al.* (SiC, Nicalon).[4] The acceptance and the progress in the silazane route have been closely connected with the name of Seyferth ever since his important contributions to this field.[5,6]

Most recent work focuses on the preparation of amorphous multinary ceramics.[7–10] These cannot be prepared using the conventional approach of the co-melting of different nitrides. One reason is the extremely low self diffusion coefficients for the corresponding cations (Si,B), another is the fact that some of the nitrides undergo decomposition into the elements prior to melting. Therefore one has to resort to an adaptation of sol–gel processing strategies in order to synthesize multinary ceramics in the system Si/B/N/C.

Our approach to multinary ceramics is characterized by two features. One corner stone of our philosophy is the use of a single source precursor molecule which already contains a M–N–M′ bridge (M,M′ = B,Si). This heteronuclear linkage mimics the desired homogeneous elemental distribution already in the precursor molecule, thus leading the way to a homogeneous material as opposed to a composite of different binary nitrides. The ceramics processed by ammonolysis of single source precursors usually exhibit superior property profiles as compared to ceramics prepared following a route in which the heteronuclear M–N–M′ linkage is not present in the precursor. Examples for this latter approach are a) co-ammonolysis of the corresponding element methylamines $M(NHCH_3)_x + M'(NHCH_3)_y$[11] or b) the hydrogen elimination approach using $M(NHCH_3)_x$ and $M'H_y \cdot NH_3$.[12] Both routes lead to Si/B/N/C ceramics which exhibit an increased tendency to crystallization and phase separation. The main advantages following these approaches is a gain in the degree of freedom for the composition, the M/M′ ratio can be varied to a large extent.

The second corner stone is the intended production of amorphous nitridic ceramics in our approach. While thermodynamically unstable as compared to the crystalline phase, the tendency toward crystallization will be minimized if the main contribution to the total enthalpy of formation lies in the covalent bonds, as is always the case in the system Si/B/N/C. The main advantage of using amorphous materials is the reduced brittleness, since no lattice planes are present to guide crack propagation.[7]

The high temperature performance[9] and the mechanical properties[13] of the ceramic have been proven to be drastically enhanced when going from ternary to quaternary ceramics. The ceramic $SiBN_3C$, processed *via* polycondensation and subsequent pyrolysis of the single source precursor TADB (trichlorosilylaminodichloroborane) remains amorphous to temperatures of $>1900\,^{\circ}C$, an increase of approx. $200\,^{\circ}C$ as compared to the ternary parent ceramic $Si_3B_3N_7$.[14] The most promising application of these ceramics involves the production of ceramic fibres *via* melt-spinning of the corresponding polymer.[7,12] These fibres exhibit a high temperature performance comparable to that of the corresponding powders and surpasses that of currently available fibres.[12]

In this contribution we will present established and new single source precursor molecules, specifically designed for the preparation of quaternary ceramics in the system Si/B/N/C. Special attention is paid to the role of carbon in improving the overall performance of the ceramics. Different possibilities for incorporating carbon into the ceramics are described and their advantages and disadvantages discussed.

The second main topic of this contribution is the structure of the final ceramics. The structural characterization of these amorphous networks is a prerequisite for an understanding of the chemical and physical properties of these materials and the fine-tuning thereof. Since the standard characterization technique, X-ray diffraction, cannot be used to elucidate structural features in these amorphous systems, other techniques have to step in.

While the short range order in the ceramics $Si_3B_3N_7$ and $SiBN_3C$ has been studied successfully using standard MAS

†Basis of a presentation given at Materials Discussion No. 3, 26–29 September, 2000, University of Cambridge, UK.

DOI: 10.1039/b002958k

NMR techniques (^{29}Si, ^{11}B, ^{15}N),[15,16] XANES spectroscopy[17,18] and X-ray and neutron diffraction techniques,[19] revealing BN_3 and SiN_4 units as the polyhedra constituting the network, the ordering on a scale down to 9 Å has been accessed by means of energy filtered transmission electron spectroscopy (EFTEM) and electron spectroscopic imaging (ESI).[20] These studies found that the ceramics $Si_3B_3N_7$ and $SiBN_3C$ are homogeneous with respect to the elemental distribution on a sub-nanometer scale. The role of carbon in these networks has been studied using advanced electron paramagnetic resonance (EPR) techniques,[16] revealing a clustering of carbon atoms. This however is in contrast to the abovementioned ESI findings.

In this contribution, MAS NMR methods are used to characterize the short and intermediate range order in the presented new ceramics.

In order to get information about the intermediate range ordering in these ceramics, that is to address the question of how the network-forming polyhedra BN_3 and SiN_4 are connected to form an extended network, we conducted ^{11}B-{^{29}Si} rotational echo double resonance (REDOR)[21–25] and ^{29}Si-{^{11}B} rotational echo adiabatic passage double resonance (REAPDOR)[26,27] experiments on the ternary model ceramic $Si_3B_3N_7$ and on the quaternary $SiBN_3C$. The combined results obtained from the different experimental approaches indicate an unexpected connectivity motif in these ceramics, characterized by regions of mainly Si–N–Si linkages and islands of predominantly B–N–B connectivities.

Of special interest is the fate of the carbon in these systems. To date, no NMR characterization of the carbon species present in the quaternary ceramics prepared by condensation of single source precursors has been possible. We will present a combination of ^{13}C MAS and advanced ^{13}C-{^{11}B} REAPDOR methods obtained on a ^{13}C isotopically enriched sample of the high performance ceramic $SiBN_3C$. These experiments comprise some evidence for at least a fraction of carbon being incorporated into the amorphous network.

Synthesis strategies and high temperature performance

The general route to the production of multinary ceramics is illustrated for the example of the synthesis of the ternary ceramic $Si_3B_3N_7$ and the quaternary ceramic $SiBN_3C$ (Fig. 1). Both are synthesized starting with the single source precursor trichlorosilylaminodichloroborane (TADB) in a two step reaction. In the first step, all chlorine groups in the precursor molecule are ammonolyzed or aminolyzed by ammonia or methylamine, resulting formally in a triaminosilylaminodiaminoborane. This change in the functionality enables the precursor molecules to undergo condensation accompanied by ammonia (or amine) elimination leading to M–NH–M′ linkages. Further condensation and polymerization is initiated thermally, resulting in the polymers polyborosilazane and *N*-methylpolyborosilazane, respectively. In a second step the polymer is pyrolyzed into the final target ceramic. At the pyrolysis temperatures (1200 °C–1400 °C) usually adopted, all organic residues and hydrogen are completely removed. It may be noticed that pyrolysis of the carbon-containing *N*-methylpolyborosilazane in a NH_3 atmosphere leads to the ternary carbon-free ceramic $Si_3B_3N_7$ indicating a polymer without extended rigid network connectivity.

Synthesis of the single source precursor TADB (Fig. 1a) has been optimized with respect to a large scale industrial production.

By far the most important characteristics for the applicability of newly synthesized ceramics is the high temperature performance. In this regard both ceramics $Si_3B_3N_7$ and $SiBN_3C$ confirm the potential of the chosen approach of synthesizing ceramics *via* polycondensation and subsequent pyrolysis of single source precursors. The resistance against oxidation, the stability towards crystallization and decomposition, often preceded by phase separation can both be studied with the help of thermogravimetry in air (resistance to oxidation) or an inert gas atmosphere (crystallization). The ternary ceramic $Si_3B_3N_7$ is stable against decomposition up to temperatures of 1700 °C,[7] the quaternary ceramic $SiBN_3C$ exhibits an even better stability up to 1900 °C.[8,14] As is found by X-ray diffraction,[7] the ceramics stay amorphous even at these high temperatures. Both ceramics exhibit an unprecedented stability against oxidation, they withstand oxidation even at temperatures of 1400 °C. Fig. 2 compares the DTA/TG curve for the TADB processed ceramic $Si_3B_3N_7$ to the corresponding curves for a composite Si_3N_4/BN and Si_3N_4, respectively. The improved high temperature performance of the ceramics obtained from single source precursors as compared to the (phase separated) composites becomes obvious and can be ascribed to the *a priori* higher atomic homogeneity. Another noticeable fact—the improvement in the high temperature performance of the quaternary carbon-containing ceramic $SiBN_3C$ relative to the ternary ceramic $Si_3B_3N_7$—indicates that the incorporation of carbon may be

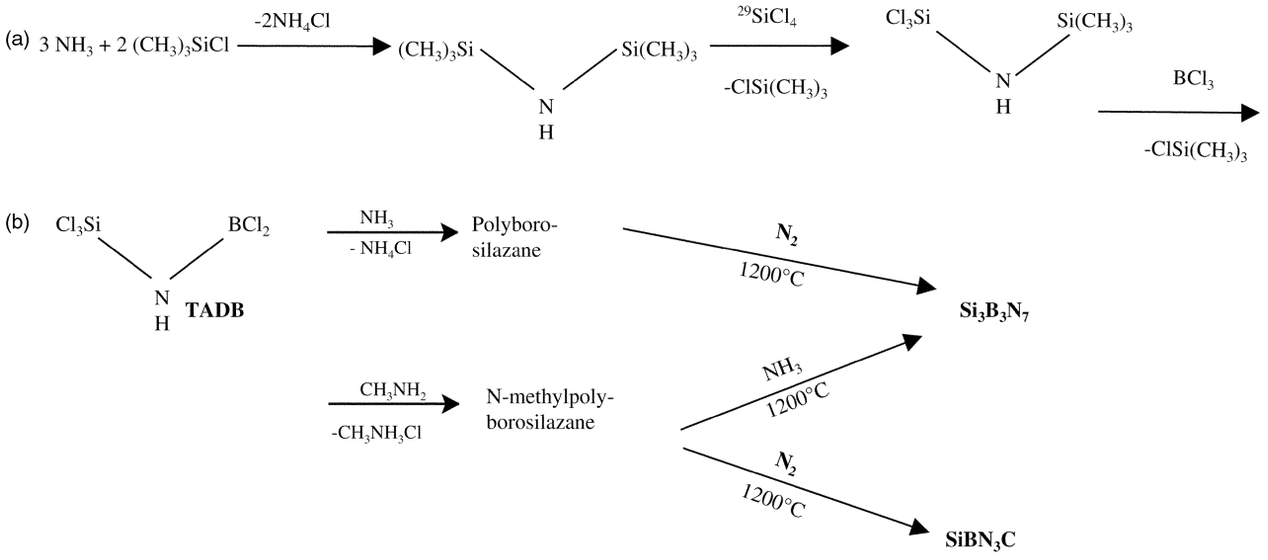

Fig. 1 a) Synthesis route to the precursor molecule TADB. b) Synthesis of the ceramics $Si_3B_3N_7$ and $SiBN_3C$.

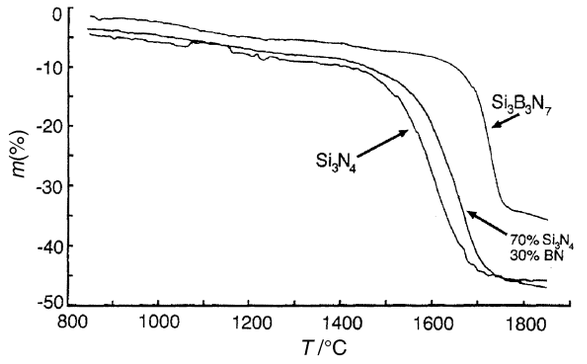

Fig. 2 High temperature TG of $Si_3B_3N_7$, a composite Si_3N_4/3BN and Si_3N_4.

responsible for this enhancement in the high temperature performance.

Even though the production of the quaternary ceramic $SiBN_3C$ has already been tailored to a large scale industrial production, these findings provide a motivation to further investigate strategies to incorporate carbon into quaternary ceramics. Principally all possible routes may be divided into four different categories, depending on the location of carbon in the single source precursor molecule or the ammonolyzer.

(a) Carbon enters the ceramic *via* the side chain of the ammonolyzer.

(b) Carbon is incorporated *via* the side chain of the single source precursor.

(c) Carbon is incorporated *via* the main chain of the ammonolyzing agent, *i.e.* C is connected to two reactive nitrogen functionalities.

(d) Carbon enters the ceramic *via* the main chain of the single source precursor molecule.

All of the routes in the reaction pathways to quaternary ceramics discussed below (Table 1) can be ascribed to at least one of these categories.

Synthesis 1 can be ascribed to category a and has already been discussed above.

Synthesis 2 utilizes the single source precursor 1-(trichlorosilyl)-1-(dichloroboryl)ethane (TSDE),[29] which is characterized by an Si–C–B linkage (category d). Ammonolysis of TSDE and subsequent pyrolysis results in the ceramic $Si_2B_2N_5C_4$. This quaternary ceramic, containing twice as much carbon with respect to silicon or boron as compared to $SiBN_3C$, exhibits a resistance against oxidation ($>1500\,^{\circ}C$) and crystallization ($>2000\,^{\circ}C$),[29] which even surpasses the characteristics of $SiBN_3C$. This finding supports the above stated hypothesis that carbon incorporation will improve the high temperature performance of the amorphous ceramics.

Synthesis 3, the reaction of TADB with cyanamide[30] as the ammonolyzing agent, is one example of a variety of tested routes in which the ammonolyzing agent is composed of at least two reactive nitrogen functions connected to a carbon atom (category c). This means that the release of carbon *via* methane or methylamine elimination during the condensation will be less likely, as is confirmed by a combination of thermogravimetry and mass spectrometry. Following the location of the carbon incorporation, carbon is expected to adopt a cationic function (in addition to silicon and boron). A variety of derivatives of carbamic acids were used as a cross-linking agent. Unfortunately, the resistance towards oxidation ($600\,^{\circ}C$–$1000\,^{\circ}C$, depending on the ammonolyzer) and the crystallization temperature ($1350\,^{\circ}C$–$1800\,^{\circ}C$) are considerably lower than those of the top ceramics $SiBN_3C$ and $Si_2B_2N_5C_4$.[30]

Syntheses 4–6 can be ascribed to category b. The single source precursor molecules methyldichlorosilylaminodichloroborane (MADB)[31] and dimethylchlorosilylaminodichloroborane (DADB)[31] contain carbon in the side chain. Consequently, the quaternary fragment C–Si–N–B is already realized in the precursor. The location of the carbon would *a priori* predict an anionic carbon in the ceramic (in addition to nitrogen). Ammonolysis of MADB with ammonia leads to an almost carbon-free ternary ceramic $SiB_{2.3}N_{3.4}$. Crosslinking of MADB and DADB with methylamine (syntheses 4 and 6) and subsequent pyrolysis results in quaternary ceramics ($SiB_{2.3}N_{2.8}C_{1.7}$ and $SiB_{3.8}N_{4.6}C_{3.3}$) in which the boron to silicon ratio is larger than unity. Silicon is obviously released during the pyrolysis process. Merely the ammonolysis of DADB with ammonia produces a quaternary ceramic with a more or less intact boron to silicon ratio. The composition of this ceramic, $SiB_{1.3}N_{2.1}C$, allows the conclusion that an average number of one methyl group per precursor molecule is released during the pyrolysis process. This ceramic exhibits the best high temperature performance among the ceramics produced by a synthesis according to category b. Decomposition does not start prior to temperatures $>2000\,^{\circ}C$, the resistance against oxidation has been confirmed to temperatures up to $1400\,^{\circ}C$.

The presented results definitely support the above mentioned hypothesis of an improved high temperature performance upon carbon incorporation. The high temperature characteristics are generally very promising except for those ceramics prepared following the route in category c, in which carbon enters the polymer connected to two reactive nitrogen sites.

Structural characterization of the ceramics

Local structure

The structural characterization of the amorphous nitridic ceramics represents one of the key issues in our work, being a prerequisite for an understanding of the physical and chemical

Table 1 Different routes to amorphous quaternary ceramics in the system Si/B/N/C

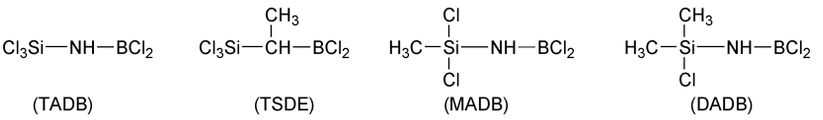

No.	Category	Single source precursor	Ammonolyzer	Ceramic[a]
1	a	(TADB)	CH_3NH_2	$SiBN_3C$
2	a,d	(TSDE)	CH_3NH_2	$Si_2B_2N_5C_4$
3	c	(TADB)	H_2N–CN	$SiBN_2C_{2.5}$
4	a,b	(MADB)	CH_3NH_2	$SiB_{2.3}N_{2.8}C_{1.7}$
5	b	(DADB)	NH_3	$SiB_{1.3}N_{2.1}C$
6	a,b	(DADB)	CH_3NH_2	$SiB_{3.8}N_{4.6}C_{3.3}$

[a]Compositions corresponding to elemental analysis except for $SiBN_3C$, the elemental analysis of which yielded $SiBN_{2.3}C_{0.8}$.[28]

properties and a fine-tuning of these characteristics. Since the absence of translatory periodicity precludes the solution of the complete structure using the standard tool, X-ray diffraction, one has to resort to other techniques. A variety of methods including XANES, neutron and X-ray diffraction, transmission electron microscopy (TEM) and nuclear magnetic resonance (NMR) spectroscopy have been used to gain some insight into the structural features of the ceramics. Magic angle spinning (MAS) NMR has emerged as the most powerful tool in the characterization of short and intermediate range ordering in amorphous networks. Conventional ^{29}Si MAS and ^{11}B MAS NMR have been used to characterize the structural units, *i.e.* the polyhedra associated with boron and silicon, present in the network. The spectra for the ceramics given in Table 1 are characterized by a remarkable similarity among each other with the exception of the ^{29}Si MAS spectrum for ceramic no. 5, $SiB_{1.3}N_{2.1}C$, which will be discussed further below. Fig. 3(top) contains representative ^{11}B MAS and ^{29}Si MAS spectra for the ceramics nos. 1–4 and 6. The ^{29}Si MAS spectra exhibit a single broad resonance centered around −45 ppm, whereas the corresponding ^{11}B MAS spectra are characterized by a powder pattern indicative of second order quadrupolar interaction. Simulation of the lineshapes results in quadrupolar coupling constants of 2.9 MHz, asymmetry parameters near 0.1 and isotropic chemical shift values of 30 ppm. The results are indicative of a trigonally planar boron coordinated by three nitrogen atoms and silicon tetrahedrally coordinated by four nitrogen atoms, as can be confirmed by comparison to the crystalline model compounds h-BN[32,33] and β-Si_3N_4.[34] This identifies BN_3– and SiN_4 units as the basic structural units of the resulting networks.

From these findings it may be concluded that the Si–C bonds in the precursor molecules MADB and DADB as well as the Si–$C(CH_3)$–B bridge, present in the precursor TSDE, are subject to cleavage under the harsh conditions employed in the pyrolysis process. Although the location of the carbon atoms in the precursor molecules principally directs carbon into anionic positions replacing nitrogen in the network, the inorganic random networks in the studied quaternary ceramics (with the exception of ceramic no. 5, $SiB_{1.3}N_{2.1}C$), are purely nitridic in their nature. Any further structural characterization has to focus on two topics: one is the intermediate range ordering motif in the quaternary ceramics; the other is the fate of carbon within these ceramics.

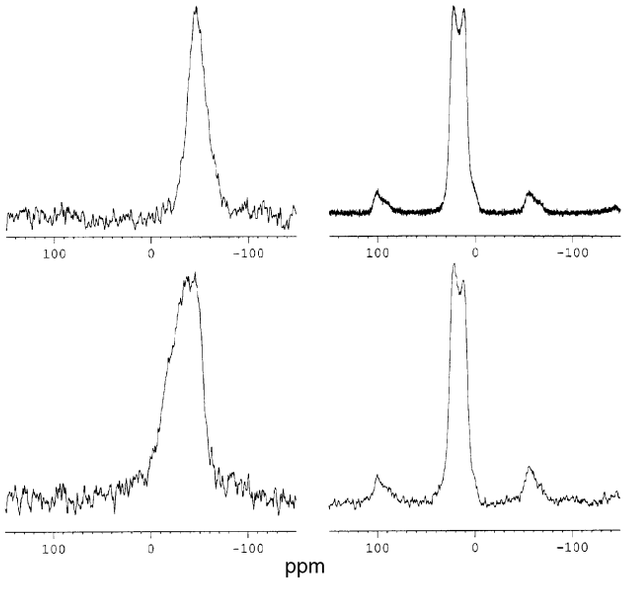

Fig. 3 Top: single pulse ^{29}Si MAS (left, $\nu_{MAS}=5$ kHz) and ^{11}B MAS (right, $\nu_{MAS}=10$ kHz) spectra for the quaternary ceramic $SiBN_3C$. Bottom: ^{29}Si MAS (left, $\nu_{MAS}=5$ kHz) and ^{11}B MAS (right, $\nu_{MAS}=10$ kHz) spectra of the ceramic no. 5, $SiB_{1.3}N_{2.1}C$. Note the difference in the ^{29}Si MAS spectra.

Intermediate range order

We chose the ternary ceramic $Si_3B_3N_7$, obtained by a pyrolysis of *N*-methylpolyborosilazane in an NH_3 atmosphere, as a starting point for the study of intermediate range ordering in the ceramics. This material is characterized by—as is the case for the quaternary ceramics—the presence of trigonally planar BN_3 and tetrahedral SiN_4 polyhedra. Using advanced double resonance NMR techniques we studied the connection of these network forming polyhedra to an extended inorganic network.

Double resonance nuclear magnetic resonance techniques such as rotational echo double resonance (REDOR)[21–25] and rotational echo adiabatic passage double resonance (REAPDOR)[26,27] spectroscopy utilize the heteronuclear dipolar coupling between the observed nucleus S and the dephasing nucleus I to obtain information about I–S internuclear distances. This information can be analyzed in terms of the number of I spins in the second coordination sphere of a central S spin.

In REDOR, the heteronuclear dipolar interaction, normally averaged out under the conditions of fast MAS, is reintroduced with the help of rotor synchronized π-pulses for the I spins. The S spin signal is observed following a rotor synchronized spin–echo sequence. In REAPDOR, a modification of REDOR, specifically designed for the study of quadrupolar nuclei as the dephasing nuclei, the dipolar coupling is reintroduced by an adiabatic rf pulse for the I spin system in the middle of the pulse sequence.

An elegant experiment providing the number of silicon atoms in the second coordination sphere of a central boron is ^{11}B-{^{29}Si} REDOR.[35] Unfortunately, this experiment is severely hampered by the low natural abundance (4.7%) of the ^{29}Si as the dephasing nucleus. Consequently, we used a 100% ^{29}Si enriched sample of $Si_3B_3N_7$ for our experiments.

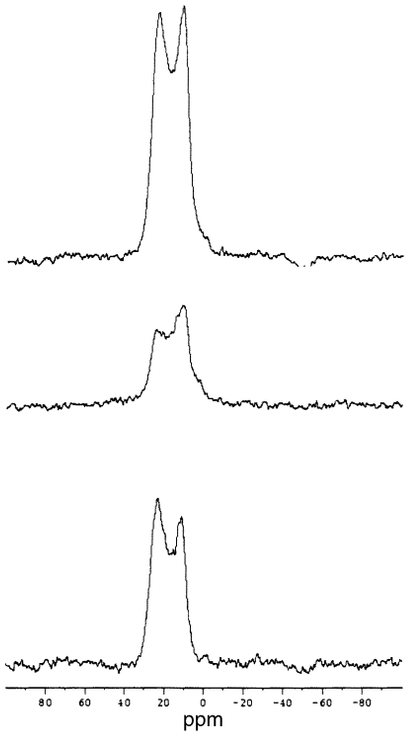

Fig. 4 Typical ^{11}B-{^{29}Si} REDOR spectra for the $Si_3B_3N_7$ ceramic. Experimental details: $\nu_{RF}(^{29}Si)=29.4$ kHz; $\nu_{RF}(^{11}B)=89$ kHz; $\nu_{MAS}=10$ kHz. Top spectrum: ^{11}B MAS spin echo spectra; middle: ^{11}B-{^{29}Si} REDOR spectrum; bottom: REDOR difference spectrum.

^{29}Si-{^{11}B} REAPDOR was used to study the second coordination sphere around a central silicon atom.[36]

Typical REDOR spectra are shown in Fig. 4. The top spectrum represents an ^{11}B MAS spin echo experiment defining the reference intensity S_0, the middle spectrum was obtained by applying additional ^{29}Si REDOR π-pulses. Dipolar dephasing leads to a decreased echo amplitude S. The bottom spectrum represents the difference S_0-S. An analogous procedure is used to obtain the ^{29}Si-{^{11}B} REAPDOR spectra. The resulting ^{11}B-{^{29}Si} REDOR curve, monitoring the second coordination sphere of a central boron atom, and ^{29}Si-{^{11}B} REAPDOR curve, monitoring the second coordination sphere around a central silicon, each obtained by plotting the MAS echo difference signal amplitudes S_0-S/S_0 as a function of the dipolar evolution time NT_R—N being the number of rotor cycles, T_R the rotor period—are shown in Figs. 5 and 6. Analysis of these double resonance curves, taking into account possible multiple spin interactions,[37–39] was performed using the simulation package SIMPSON.[40] Extensive simulations revealed[36,38] that in the case of multiple spin interactions and distribution effects only the initial part of the dipolar evolution curves, up to $\Delta S/S_0 \cong 0.6$ should be used for the simulations. A crucial parameter is the B–Si internuclear distance, which we assumed to be 2.74 Å, a value, suggested by evaluation of neutron diffraction data.[19] A single B–Si dipolar interaction produces the dashed lines in Figs. 5 and 6. In the case of the ^{29}Si-{^{11}B} REAPDOR experiment, the natural abundance of the ^{11}B isotope (80%) has to be taken into account. Simulation of a three-spin interaction (BSi_2 for the REDOR curve and SiB_2 for the REAPDOR curve) produces the dotted lines in Figs. 5 and 6. The ^{11}B-{^{29}Si} REDOR data can be simulated using a superposition of the curves corresponding to the BSi and BSi_2 interaction according to $\Delta S/S_0 = 0.44\Delta S/S_0$ (BSi_2) $+ 0.56\Delta S/S_0$ (BSi). This corresponds to an average number of 1.4 silicon atoms in the second coordination sphere around a central boron atom.

In a similar vein, the ^{29}Si-{^{11}B} REAPDOR data is consistent with a superposition of SiB and SiB_2 interactions according to 1.8 boron neighbors in the second coordination sphere around a central silicon atom. These findings indicate that the inorganic network realized in the ceramic $Si_3B_3N_7$ is not characterized by a homogeneous elemental distribution (this would lead to four boron atoms in the second coordination sphere of a silicon site and three silicon

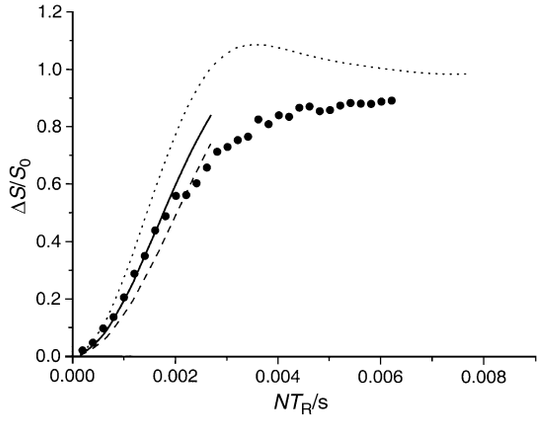

Fig. 5 Experimental ^{11}B-{^{29}Si} REDOR data together with simulated REDOR dephasing curves under the assumption of a) one single B–Si dipolar coupling, $d = 2.74$ Å (dashed line); b) two B–Si dipolar couplings, $d = 2.74$ Å (three-spin system BSi_2); α (the angle between the two B–Si internuclear vectors) = 66° (dotted line) and c) weighted superposition of a) and b) according to $\Delta S/S_0 = 0.44\Delta S/S_0$ (BSi_2) $+ 0.56\Delta S/S_0$ (BSi) (solid line). Experimental details: $\nu_{RF}(^{29}Si) = 29.4$ kHz; $\nu_{RF}(^{11}B) = 89$ kHz; $\nu_{MAS} = 10$ kHz.

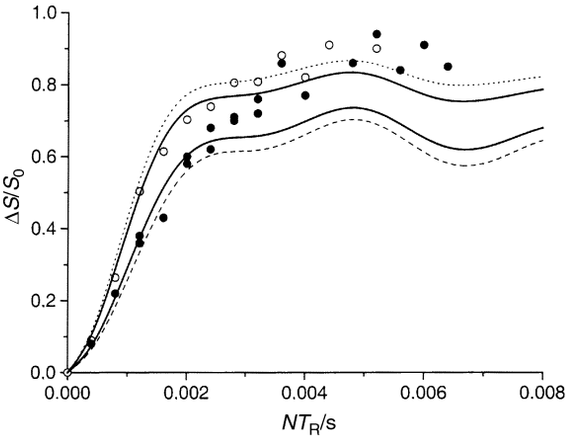

Fig. 6 Experimental ^{29}Si-{^{11}B} REAPDOR curves for $Si_3B_3N_7$ (open circles) and $SiBN_3C$ (filled circles). Dashed line: REAPDOR dephasing calculated for a single ^{29}Si-{^{11}B} dipolar coupling. Dotted line: REAPDOR dephasing curves calculated for a SiB_2 three-spin system with $\alpha = 54°$. Note that the dephasing curve for the SiB_2 three-spin system is actually a superposition of the dephasing curves for a two-spin and a three-spin interaction due to the natural abundance of the ^{11}B isotope (80.4%). Solid lines: weighted superposition of the REAPDOR curves for a SiB interaction and a SiB_2 interaction according to $\Delta S/S_0 = 0.512\Delta S/S_0$ (SiB_2) $+ 0.416\Delta S/S_0$ (BSi) for $Si_3B_3N_7$ (corresponding to 1.8 boron neighbors in the second coordination sphere of silicon) and to $\Delta S/S_0 = 0.128\Delta S/S_0$ (SiB_2) $+ 0.704\Delta S/S_0$ (BSi) for $SiBN_3C$, corresponding to 1.2 boron atoms in the second coordination sphere of silicon. Experimental details: $\nu_{RF}(^{29}Si) = 29.4$ kHz; $\nu_{RF}(^{11}B) = 89$ kHz; $\nu_{MAS} = 5$ kHz.

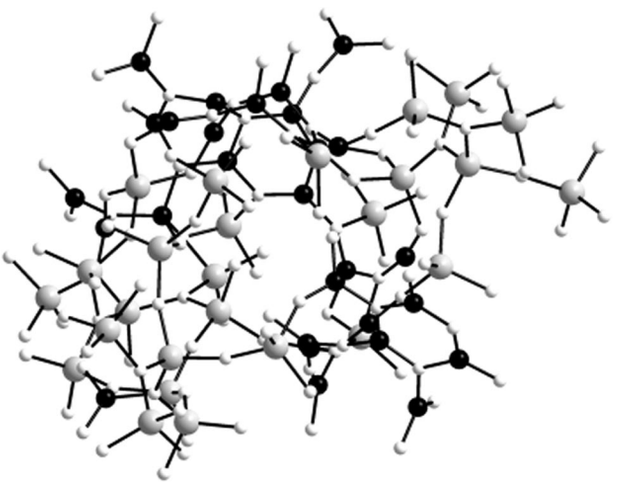

Fig. 7 Proposed structural model for the $Si_3B_3N_7$ ceramic.

atoms in the second coordination sphere of a central boron). The network adopted is governed by the presence of Si–N rich islands and B–N rich domains, respectively. An illustration of this network is given in Fig. 7. The reason for this obvious avoidance of Si–B–N connectivity may be found in the kinetics of the ammonolysis and condensation step of the synthesis. The B–Cl bonds are expected to be attacked by ammonia or methylamine much faster than the competing Si–Cl bonds due to the higher Lewis-acidity of the BCl_2 fragment. Thus, only B–NH_2 groups are available for polycondensation during the initial steps of the polymerisation. Si–Cl bonds are not attacked unless the local B–Cl supply is almost depleted.

The role of carbon in the quaternary ceramics

The most important question is the fate of carbon in the quaternary ceramics. The increase in the high temperature performance going from $Si_3B_3N_7$ to $SiBN_3C$ (Fig. 2) must be

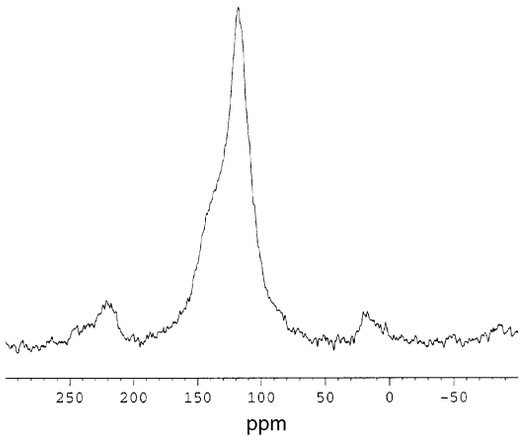

Fig. 8 ^{13}C MAS spectrum for ceramic no. 1, $SiBN_3C$. $\nu_{MAS} = 10$ kHz.

somehow related to the presence of carbon. It is still an open discussion whether carbon participates in the network construction or is consumed in graphite-like regions, thus producing a composite with the ternary phase $Si_3B_3N_7$. While the exclusive presence of BN_3 and SiN_4 polyhedra in the ceramics 1–4 and 6 excludes any anionic carbon—replacing nitrogen within the network—carbon may well be incorporated within the cationic positions, replacing silicon and boron.^{13}C MAS NMR is expected to assist in the assignment of the carbon location, but, unfortunately, to date, it has not been possible to acquire a ^{13}C MAS NMR spectrum of the quaternary ceramics obtained by condensation and subsequent pyrolysis of single source precursors. We consequently used a sample of $SiBN_3C$, 15% isotopically enriched in ^{13}C (using a mixture of CH_3NH_2 and $^{13}CH_3NH_2$ for the condensation).[31] The corresponding ^{13}C MAS spectrum is shown in Fig. 8. Two signals can be identified, a rather broad component centered around 130 ppm and a narrow line with an isotropic chemical shift of 115 ppm. While the isotropic chemical shift values assign both signals to sp^2 hybridized carbon, no information about the position within the ceramic is obtained. This can be studied with the help of the double resonance experiments described above. Apart from ^{13}C-$\{^{29}Si\}$ REDOR, which is not feasible due to the low natural abundance of the ^{29}Si isotope, the most promising approach to the end of identifying the fate of carbon is to perform a ^{13}C-$\{^{11}B\}$ REAPDOR experiment. Fig. 9 reveals the REAPDOR spectra for a dipolar evolution time of 1.6 ms. The difference spectrum (Fig. 9, bottom) obviously contains no contribution from the narrow signal at 115 ppm. This allows the conclusion that the carbon atoms producing the narrow signal are well separated from the boron atoms within the network, whereas the broad component, which definitely shows dipolar dephasing, represents carbon atoms which are part of the network. The resulting ^{13}C-$\{^{11}B\}$ REAPDOR curve is given in Fig. 10. Solid lines correspond to theoretical REAPDOR curves assuming the C–B distances indicated. The $\Delta S/S_0$ values plotted in Fig. 10 were obtained by integrating the complete signal, since a deconvolution into two individual lines proved to be unsuccessful because of the low signal to noise ratio. This leads to an inherent underestimation of the actual dipolar coupling, since a fraction of the integrated signal, the narrow line, does not contribute to the dipolar dephasing. Thus, the estimated B–C internuclear distances are too large. Taking these considerations into account, the REAPDOR data can be interpreted in terms of C–N–B connectivity in the amorphous network, although no quantification of our results is possible at this point. Support for the incorporation of carbon into the network can be obtained by analyzing the ^{29}Si-$\{^{11}B\}$ REAPDOR data for the ceramic

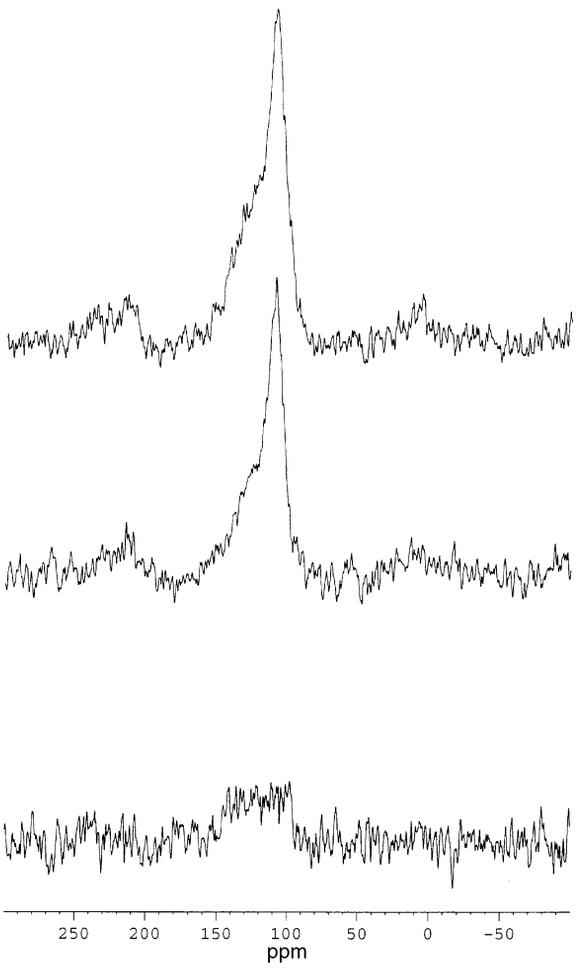

Fig. 9 ^{13}C-$\{^{11}B\}$ REAPDOR spectra for ceramic no. 1, $SiBN_3C$. Note that in the difference spectrum no contribution from the narrow signal at 115 ppm can be identified.

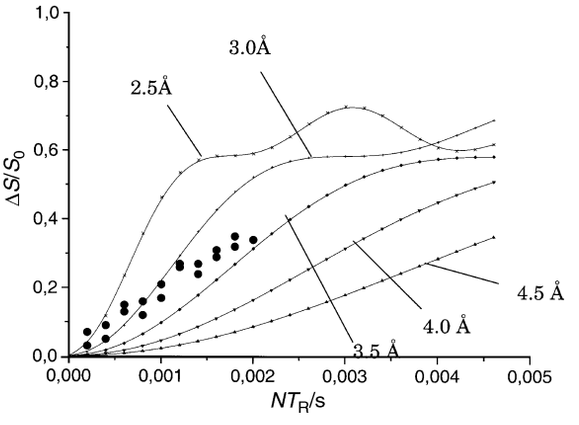

Fig. 10 ^{13}C-$\{^{11}B\}$ REAPDOR curve for $SiBN_3C$ together with simulations assuming the ^{13}C–^{11}B internuclear distances indicated.

$SiBN_3C$, shown as filled circles in Fig. 6. Calculations as described for the ternary ceramic $Si_3B_3N_7$ lead to an averaged number of 1.2 boron atoms in the second coordination sphere of boron. Assuming the general network structure to be similar to the corresponding ternary network, the missing boron atoms may have been replaced by carbon.

The carbons associated with the narrow line obviously do not experience any dipolar coupling to boron nuclei. The location of this type of carbon still has to be determined.

Ceramic no. 5, $SiB_{1.3}N_{2.1}C$, processed by condensation of DADB in ammonia, is characterized by a unique structural

motif among these ceramics. The ^{29}Si MAS resonance line (Fig. 3, bottom), centered around −36 ppm, reveals the presence of structural units of the general form SiN_xC_y.[41] The lineshape may be deconvoluted into three individual gaussians (not shown) with isotropic chemical shifts of −22 ppm, −37 ppm and −46 ppm. These can be assigned to SiN_2C_2 (−22 ppm), SiN_3C (−37 ppm) and SiN_4C_0 (−46 ppm) units, each with equal probability. Obviously carbon participates in the network, adopting an anionic function, thus replacing part of the nitrogen. A network comprised of silicon and boron occupying the cationic sites and carbon and nitrogen sharing the anionic positions, is adopted. Further characterization of the structural details of this very promising material is necessary to elucidate the nature of this quaternary network.

Conclusions

Different routes to the incorporation of carbon into inorganic random networks in the system Si/B/N/C were presented. Of the different ways of potentially incorporating carbon into the anionic positions of the network (routes b and d) only the condensation of DADB with ammonia and subsequent pyrolysis in a nitrogen atmosphere is successful, as is confirmed by ^{29}Si MAS NMR. The fate of carbon incorporated into the cationic positions of the network, replacing silicon and boron, was traced using advanced NMR double resonance techniques. The results presented give some evidence for carbon being directly incorporated (at least partially) into the amorphous network. Analyzing the ^{11}B–^{29}Si double resonance experiments, a structural model is emerging in which the random network is dominated by BN_3 and SiN_4 polyhedra. The intermediate range order is characterized by an agglomeration of B–N–B linkages and Si–N–Si linkages to form boron-rich and silicon-rich domains. Carbon enters the network on the cationic positions, replacing silicon and boron. This model may explain the enhanced durability and high temperature performance at the transition from the ternary Si–B–N network in $Si_3B_3N_7$ to the quaternary networks in $SiBN_3C$, $Si_2B_2N_5C_4$ and related ceramics.

References

1 P. Chantrell and E. P. Popper, in *Special Ceramics*, E. P. Popper ed., Academic Press, NY, 1964, p. 87.
2 G. Winter, W. Verbeek and M. Mansmann, *Chem. Abstr.*, 1974, **81**, 126134.
3 H. Lange, G. Wötting and G. Winter, *Angew. Chem.*, 1991, **103**, 1606.
4 S. Yajima, J. Hayashi and M. Omori, *Chem. Lett.*, 1975, 931.
5 D. Seyferth and G. H. Wiseman, *Ultrastruct. Process. Ceram. Glasses Compos. Proc. Int. Conf.*, 1984, **265**, 27.
6 D. Seyferth, G. H. Wiseman and C. Prudhommes, *J. Am. Ceram. Soc.*, 1983, **66**, C13.
7 H. P. Baldus and M. Jansen, *Angew. Chem., Int. Ed. Engl.*, 1997, **36**, 328.
8 M. Jansen, *Solid State Ionics*, 1997, **101–103**, 1.
9 M. Jansen and H. Jüngermann, *Curr. Opin. Solid State Mater. Sci.*, 1997, **2**, 150.
10 P. Baldus, M. Jansen and D. Sporn, *Science*, 1999, **285**, 699.
11 J. Löffelholz, J. Engering and M. Jansen, *Z. Anorg. Allg. Chem.*, 2000, **626**, 963.
12 J. Löffelholz and M. Jansen, *Adv. Mater.*, 1995, **7**, 289.
13 H. P. Baldus, G. Passing, H. Scholz, D. Sporn, M. Jansen and J. Göring, *Key Eng. Mater.*, 1997, **127–131**, 177.
14 H. P. Baldus, O. Wagner and M. Jansen, *Mater. Res. Soc. Symp. Proc.*, 1992, **271**, 821.
15 U. Müller, W. Hoffbauer and M. Jansen, *Chem. Mater.*, 2000, in press.
16 G. Jeschke, M. Kroschel and M. Jansen, *J. Non-Cryst. Solids*, 1999, **260**, 216.
17 R. Franke, St. Bender, H. Jüngermann, M. Kroschel and M. Jansen, *J. Electron Spectrosc. Relat. Phenom.*, 1999, **101–103**, 641.
18 R. Franke, St. Bender, I. Arzberge, J. Hormes, M. Jansen, H. Jüngermann and J. Löffelholz, *Fresenius Z. Anal. Chem*, 1996, **354**, 874.
19 R. M. Hagenmayer, U. Müller, C. J. Benmore, J. Neuefeind and M. Jansen, *J. Mater. Chem.*, 1999, **9**, 2865.
20 D. Heinemann, W. Assenmacher, W. Mader, M. Kroschel and M. Jansen, *J. Mater Res.*, 1999, **14**, 3746.
21 T. Gullion and J. Schaefer, *J. Magn. Reson.*, 1989, **81**, 196.
22 T. Gullion, *Magn. Reson. Rev.*, 1997, **17**, 83.
23 Y. Pan, T. Gullion and J. Schaefer, *J. Magn. Reson.*, 1990, **90**, 330.
24 T. Gullion, *J. Magn. Reson.*, 1995, **117**, 326.
25 L. van Wüllen, B. Gee, L. Züchner, M. Bertmer and H. Eckert, *Ber. Bunsen-Ges. Phys. Chem.*, 1996, **100**, 1539.
26 T. Gullion, *J. Magn. Reson.*, 1995, **A117**, 326.
27 L. Chopin, S. Vega and T. Gullion, *J. Am. Chem. Soc.*, 1998, **120**, 4406.
28 S. Mann, D. Geilenberg, J. A. C. Broekaert and M. Jansen, *J. Anal. At. Spectrom.*, 1997, **12**, 975.
29 H. Jüngermann and M. Jansen, *Mater. Res. Innovations*, 1999, **2**, 200.
30 H. Jüngermann and M. Jansen, *Materwiss. Werkstofftech.*, 1998, **29**, 573.
31 U. Müller and M. Jansen, PhD thesis, Bonn, 2000.
32 A. H. Silver and P. J. Bray, *J. Chem. Phys.*, 1960, **32**, 288.
33 G. Jeschke, W. Hoffbauer and M. Jansen, *Solid State NMR*, 1998, **12**, 1.
34 K. R. Carduner, C. S. Blackwell, W. B. Hammond, F. Reidinger and G. R. Hatfield, *J. Am. Chem. Soc.*, 1990, **112**, 4676.
35 L. van Wüllen, U. Müller and M. Jansen, *Angew. Chem.*, 2000, **112**, 2574; L. van Wüllen, U. Müller and M. Jansen, *Angew. Chem., Int. Ed.*, 2000, **39**, 2519.
36 L. van Wüllen and U. Müller M. Jansen, *Chem. Mater.*, 2000, in press.
37 A. Naito, K. Nishimura, S. Tuzi and H. Saito, *Chem. Phys. Lett.*, 1994, **229**, 506.
38 J. C. Chan, M. Bertmer and H. Eckert, *J. Am. Chem. Soc.*, 1999, **121**, 5238.
39 J. M. Goetz and J. Schaefer, *J. Magn. Reson.*, 1997, **117**, 147.
40 M. Baks, J. T. Rasmussen and N. C. Nielsen, *40th Experimental Nuclear Magnetic Resonance Conference*, Orlando, 1999.
41 C. Gerardin, M. Henry and F. Taulelle, *Mater. Res. Soc. Symp. Proc.*, 1992, **271**, 777.